J. Anal. Appl. Pyrolysis 82 (2008) 235–239

Contents lists available at ScienceDirect

Journal of Analytical and Applied Pyrolysis

journal homepage: www.elsevier.com/locate/jaap

Chemical structural characterization of pyrolyzed and subsequently ion-implanted poly(acrylonitrile)

Shehdeh Jodeh *

Department of Chemistry, Najah National University, P.O. Box 7, Nablus, Palestine

ARTICLE INFO

Article history:
Received 6 August 2007
Accepted 25 March 2008
Available online 4 April 2008

Keywords:
Poly(acrylonitrite)
Polyconjugated
Pyrolysis
Heat treatment

ABSTRACT

Infrared (IR), Auger electron spectroscopy (AES) and X-ray photoelectron spectra (XPS) of pristine, pyrolyzed, and ion-implanted poly(acrylonitrite) (PAN) samples were obtained in order to correlate the structural changes accompanying pyrolysis and implantation with the electrical properties of the respective PAN products. The results show that PAN is first converted to a polyconjugated heterocyclic ladder structure at a temperature of 435 °C and then to a graphite-like structure at temperature above 750 °C. Pyrolysis studies took place in a temperature range of 350–750 °C. IR studies showed that upon heat treatment at 435 °C, major structural changes occur as indicated by the complete disappearance of the nitrile and methylene absorption bands and the formation of new bands. The degree of conjugation in pyrolyzed PAN can be selectively controlled by the proper choice of the heat treatment temperature. From the studies, ion implantation causes extensive nitrogen depletion and the nitrogen chemical state in the implanted sample is different from that found in the pyrolyzed materials. Upon ion implantation, the component assigned to the nitrogen in a sigma bonding state (401.27 eV) increased in intensity (46%) relative to the intensity (27%) of the component for which nitrogen is in a hetroaromatic structure. Both AES and XPS analysis showed the variation of C:N ratio as a function of heat treatment.

1. Introduction

Carbon fibers and activated carbon fibers are produced by carbonizing a raw material such as poly(acrylonitrite) (PAN) fiber [1,2]. Carbon fibers are excellent reinforced materials for composites, are now important industrially and have gained a wide range of applications in the industrial and engineering fields, from sport articles to the aerospace industry [3,4]. Activated carbon fibers have received increasing attention in recent years as an absorbent, filter, etc. for filtering automobile gasoline, deodorizing tobacco smoke, recovering solvents and purifying water [5–7]. PAN fibers have been found to be the most suitable precursors for making high-performance carbon fiber [8–10].

For instance, the preparation of semi-conducting carbon fiber by pyrolysis of PAN precursors has been described [11].

An important step in preparing carbon fiber from the PAN fiber is to heat the precursor at 200–300 °C in air or in an oxygen-containing atmosphere, i.e., the stabilization of fiber. Subsequently, carbonization and graphitization is carried out at higher temperature in an inert atmosphere to obtain a particular type of carbon fibers. The reaction steps involved in the formation of stabilized PAN (fibers) have been studied and confirmed by several authors [4,8,12,13,14–19]. During subsequent carbonization in a non-oxidizing atmosphere, oxygen atoms and hetrocydic nitrogen are split off and planar polyaromatics are formed. All these stabilization and carbonization reactions result in volatile by products according to the previous results of Fitzer et al. [4]. Some mass loss from chain scission and elimination of HCN and NH_3 accompanies the cyclization reactions [8]. Oxygen, which is added and is present during stabilization, is mostly present as –OH and C═O groups. However, some authors have suggested that oxygen attached to the imines nitrogen atoms to give a nitrone (N–O) moiety based on infrared spectroscopy and model compound studies [20–22].

In other studies when PAN-based products were considered, contrary to the trends observed for pure PAN, evolution of HCN and the degradation products due to the hemolytic cleavages of the polymer backbone continued throughout the pyrolysis indicating a significant increase in their production even at the final stages of pyrolysis [23]. On the other hand, the yield of thermal degradation products associated with decomposition of the unsaturated cyclic imines segments decreased. Although doping by ion implantation has not been applied to polymers until late 1980s, current findings have shown that conductivity values as high as 10 $\Omega\,cm^{-1}$ can be

* Tel.: +972 9 299 5744; fax: +972 9 234 7488.
E-mail address: sjodeh@hotmail.com.

0165-2370/$ – see front matter © 2008 Elsevier B.V. All rights reserved.
doi:10.1016/j.jaap.2008.03.014

obtained in certain polymers using this technique [24]. Vankatesan et al. compared the properties of products obtained from pyrolysis and from ion implantation of polymeric and carbon films and concluded that there are two different modes of energy deposition that have similar effects on these materials [25]. X-ray photoelectron spectra (XPS) and Raman analysis suggest that the observed improvement were due to the formation of a substantial amount of hydrogenated amorphous carbon phase in the polymer surface. Other studies showed that silver ions between 5 and 30 keV implanted into polystyrene at a constant dose of 3×10^{15} ions/cm^2 encouraged human umbilical vascular endothelial cell growth and proliferation, whilst no growth was observed on untreated samples [26]. The effect increased with increasing ion energy up to 20 keV, but decreased at 30 keV, closely following the water contact angle measurements.

This study describes the effects of both pyrolysis and ion implantation on thin poly(acrylonitrite) films prepared and purified by dissolution in *N*,*N*-dimetly-formamide (DMF) and reprecipitation with distilled water. This study will help us to understand aims at clarifying the effect of structural modification on the electrical conductivity of poly(acrylonitrite) applications in automotive industries which will be studied separately in the future. Infrared ATR-IR, Auger electron spectroscopy (AES) and XPS instruments were used to understand the structure modification after pyrolysis and ion implantation of poly(acrylonitrite).

2. Experimental

Poly(acrylonitrite) was obtained from the Aldrich Chemical Company. It was purified by dissolution in DMF at 80 °C and reprecipitation with distilled water. The purified material was then dried at 80 °C in a vacuum oven for a period of 72 h. Thin films of PAN were prepared by spin coating from a solution of purified PAN in DMF. In the experiments involving spectroscopic analysis, PAN thin films were coated onto a platinum film (0.1 μm) evaporated over a 1-μm layer of thermally grown SiO_2 on a silicon substrate. The desired thickness of PAN films was obtained by controlling the spinning speed, duration of spinning, and the concentration of the solution. Film thicknesses (0.3–1 μm) were measured after pyrolysis or ion implantation using a number of techniques such as surface profilometry, Rutherford backscattering spectrometry, and Auger electron spectroscopy. The results of measurements obtained by these different techniques were in agreement. In the pyrolysis experiments, the deposited PAN films were dried in a vacuum oven at room temperature for a period of 48 h. They were then moved to a tubular furnace (2 in. in diameter) and placed under a dynamic vacuum of 1×10^{-6} Torr for 4 h at room temperature. To evaporate the residual solvent, the temperature of the tube was raised to 80 °C and maintained at that level for a period of 15–20 h. This is followed by additional heating at 200 °C for a period not exceeding 3 h. After complete removal of the solvent, the samples were pyrolyzed under vacuum at the desired temperature. The selected pyrolysis temperatures were 350, 435, 550, 650, and 750 °C and the corresponding samples were labeled as PAN350, PAN435, PAN550, PAN650, and PAN750 in order to designate their respective pyrolysis temperatures.

Additional sets of pyrolyzed PAN were prepared and were ion implanted with arsenic at an energy level ranging between 50 and 200 keV and at doses of 5×10^{14} to 5×10^{16} ions/cm^2. The implantation was performed at room temperature with the ion beam directed normal to the film surface. The ion beam current density was less than l μA/cm^2 in order to minimize target heating. The depth distribution of the ions was determined by Auger spectroscopy as a function of argon sputtering time. A typical result is presented in Fig. 1 for a PAN435 sample implanted with arsenic at

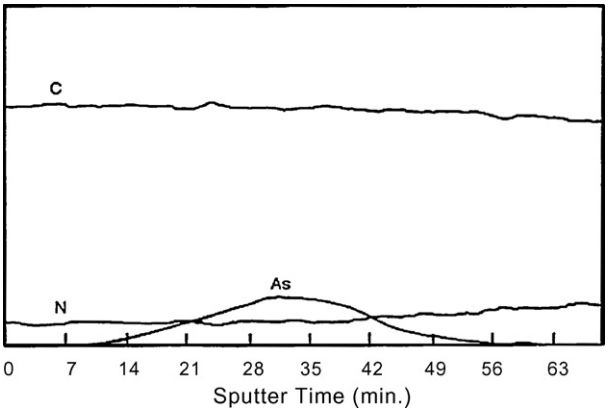

Fig. 1. Auger depth profile of arsenic implanted PAN435. Sputtering rate is 65 Å/min.

200 keV and 1×10^{16} ions/cm^2, based on analysis of the 376 eV arsenic Auger transition. A crude estimate of the sputtering rate for the polymer was made by comparison with the sputtering rate of a chemically grown Ta_2O_5 layer. The results of Fig. 1 show a Gaussian profile, as expected from the LSS theory, and the measured ion penetration depth (Rp ∼2200 Å) is in good agreement with the theoretical value [27]. For convenience the ion-implanted samples have been labeled with a letter I preceded by the temperature at which the sample was pyrolyzed before implantation, e.g., PAN435I represents a sample pyrolyzed at 435 °C then ion implanted.

The pyrolyzed and the ion-implanted PAN samples were characterized using ATR-FTIR spectrometry, electron spectroscopy for chemical analysis (ESCA or XPS) and AES. The FTIR spectra were obtained by internal reflectance with a 60° germanium crystal using a Nicolet 5 DXB FTIR spectrometer. The ESCA and the AES spectra were recorded using a PerkinElmer model 549 ESCA/SAM electron spectrometer. Depth profile analyses for the ion-implanted samples were performed by sputtering with a 2-keV argon ion beam.

3. Results and discussion

Infrared ATR-IR, AES and XPS of pristine, pyrolyzed, and ion-implanted PAN samples were obtained in order to correlate the structural changes accompanying pyrolysis and implantation of PAN products. Fig. 2 shows the IR spectra of pristine PAN and of PAN films pyrolyzed at different heat-treatment temperatures (435 °C, PAN435; 750 °C, PAN750). The spectrum of pristine PAN Fig. 2a shows a sharp absorption at 2242 cm^{-1} characteristic of the nitrile group (C≡N). The absorptions at 1452, 1359, and ∼3000 cm^{-1} are associated with the methylene bending and stretching vibrations [28]. Upon heat treatment at 435 °C, major structural changes occur as indicated by the complete disappearance of the nitrile and the methylene absorption bands and the formation of new bands at 1600 and 1375 cm^{-1} (Fig. 2b). These bands are associated with chain conjugation through the formation of (C=C) and (C=N) bonds [29]. Broadening of the absorption bands in the 1300–1600 cm^{-1} range upon heating at 750 °C (Fig. 2d) is indicative of extensive conjugation in the system. Thus, the degree of conjugation in pyrolyzed PAN can be selectively controlled by the proper choice of the heat-treatment temperature. The control of the efficiency of conjugation is of primary importance, not only from the point of view of thorough understanding of the nature of the phenomenon but also as a means of controlling the electrical, thermal, mechanical and other properties of the pyrolyzed product.

The IR spectrum (Fig. 2c) of PAN pyrolyzed at 435 °C and then ion implanted with arsenic (PAN435I) exhibited broad absorption

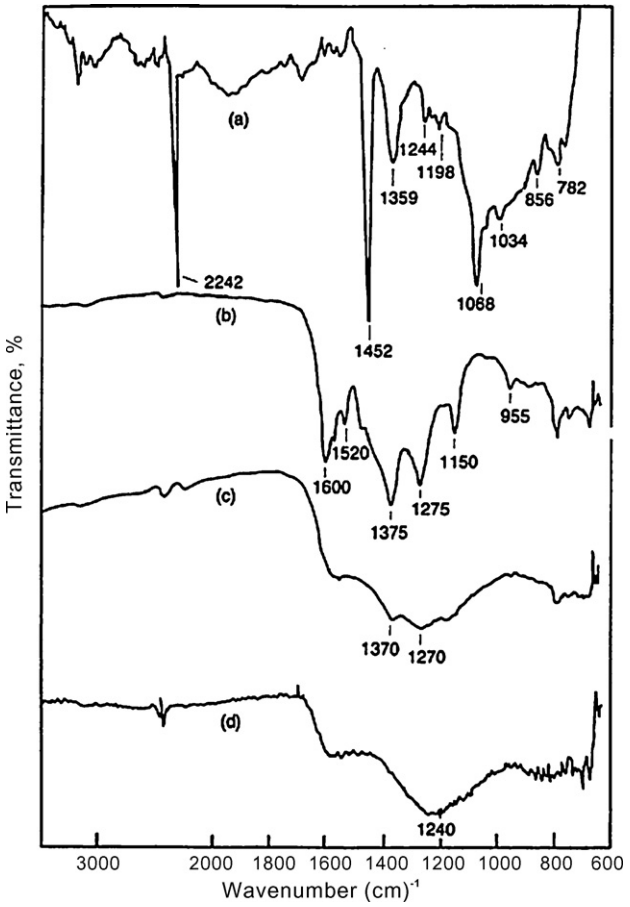

Fig. 2. ATR-FTIR spectra of (a) PAN, (b) PAN435, (c) PAN435I, and (d) PAN750.

features similar to those of PAN pyrolyzed at 750 °C. The superimposed bands at 1270, 1370, and 1600 cm^{-1} are due to functional groups (primarily C═N and C═C bonds) characteristic of the parent pyrolyzed material (PAN435) remnant of which, presumably, exists after implantation. The broad overlapping absorptions in the spectra of both PAN750 and PAN435I are consistent with a fused aromatic structure (carbonization). However, a detailed quantitative description of that structure cannot be made on the basis of such data.

Electron spectroscopy for chemical analysis and AES provided additional information regarding the structures of pyrolyzed and ion-implanted PAN. Both XPS and AES spectra displayed signals due to C ls, N ls and O ls core electrons. The intensities of these signals were a function of the treatment history of PAN. The oxygen signal is due to surface oxidation of the heat treated and ion-implanted samples. Sputtering of a 50-Å layer from the surface is accompanied by a complete disappearance of the oxygen signals.

The changes in the elemental composition associated with heat treatment and with ion implantation of PAN are presented in Table 1. The pristine PAN show: a C:N ratio of 3.3 as expected from the molecular structure (3C:1N). Upon heat treatment, a progressive increase in the carbon content is observed as the heat treatment is raised from 350 to 750 °C. This is accompanied by a decrease in the nitrogen content of the samples.

More important in this analysis is the variation in the C:N ratio as a function of heat treatment (Table 1). At 350 °C, the pyrolyzed sample displayed a C:N ratio of 6:1. As the heat treatment is raised to 435 °C, (PAN435), the C:N ratio dropped to a value of 4.4. The difference is due to the thermal elimination at 350 °C of compounds, such as HCN and C_2N_2, having a C:N ratio lower than the characteristic ratio (3:1) of PAN polymer [30]. In other words, there is a greater loss in the nitrogen content relative to that of the carbon at 350 °C. As the heat treatment is raised to 435 °C, large molecules of a higher C:N ratio are eliminated (acrylonitrile, vinylacetonitrile) leading to the observed decrease in the C:N ratio [31]. Heat treatment at 750 °C resulted in a dramatic drop in the nitrogen content yielding a C:N ratio of 9:1, consistent with the pyrolysis scheme depicted in previous studies [31].

The XPS core level C 1s spectra of pristine, heat treated and ion-implanted PAN samples are given in Figs. 3–5. All of the C ls and N ls spectra were fitted by Gaussian component peaks. Carbon and nitrogen atoms can form at least three different chemical bonds: C–N, C═N, and C≡N. An image of the chemical configuration of nitrogen and carbon atoms in the films can be deduced from the deconvolution of the individual C 1s and N 1s lines into Gaussian line shapes. This deconvolution is somehow critical because of the experimental resolution in comparison with the close values of binding energy of the several components. The C 1s core level showed two signals; one at 285.5 eV (CH_2) and strong peak at 286.5 eV (CHCN).

However, it is generally observed that with increasing nitrogen concentration in the CN_x films, the C 1s peak broadens and becomes more asymmetric which we do not see in Fig. 3a. In

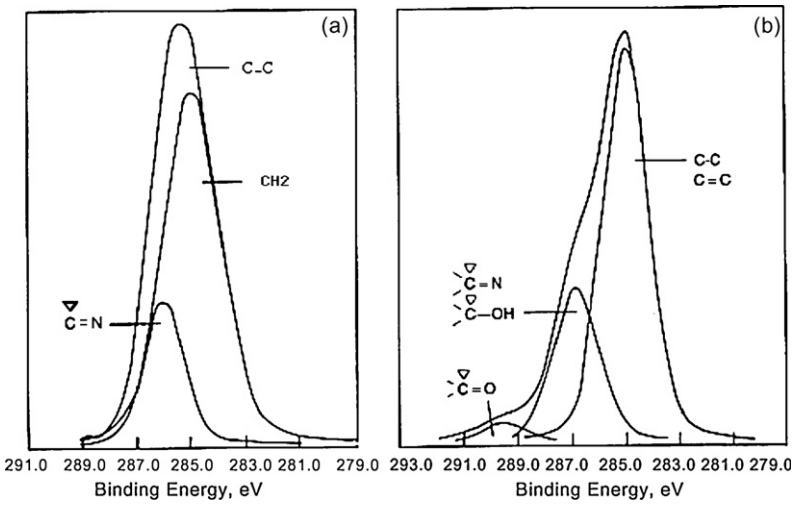

Fig. 3. Curve-resolved XPS C 1s of (a) PAN and (b) PAN435.

Table 1
XPS semi-quantitative elemental composition analysis (atomic percent)

Sample	C	N	O	C/N
PAN	76	23	1.0	3.3:1
PAN350	72	12	16.0	6.0:1
PAN435	74	17	9.0	4.4:1
PAN750	81	9	10.0	9.0:1
PAN435I	87	2	11.0	44.0:1

Table 2
The percentage of chemical states of carbon bonding in pyrolyzed and ion-implanted PAN

Sample	CC	CN	CO	CC/CN
PAN	76	34	–	2.2:1
PAN350	71	23	6	3.1:1
PAN435	70	27	3	2.6:1
PAN750	76	18	6	4.2:1
PAN435I	77	16	7	4.8:1

(Fig. 3a), the Cls parameters (position and f.w.h.m) of hydrocarbons were used as a reference. The hydrocarbon Cls binding energy was taken to be 285.5 eV in the curve fitting process [32]. The position and intensity of the other peaks (e.g., C≡N) were then optimized to give the best fit to the experimental spectrum maintaining the same f.w.h.m as the main component. The curve fitted C ls and N ls peaks are also given in Figs. 3–5. Both the C ls and the N ls peaks broaden upon pyrolysis (or ion implantation) indicating the formation of various new chemical species. The C ls spectra are complicated by the contribution of carbon atoms having chemical structures associated with the surface oxidation of the material (C═O, C–OH). In the direction of increasing binding energy, the Cls peaks are assigned to hydrocarbon, C═N and C–OH, and C═O bonds, respectively [33].

Table 2 gives the proportions of the various carbon structures found in the samples, as calculated from the corresponding Cls peak areas. It is clear that heat treatment of PAN increases the carbon-to-carbon bonding at the expense of carbon to nitrogen bonds.

The contributing factors are the heat-induced elimination of small molecules (containing nitrogen) and the formation of aromatic non-heterocyclic fused ring structures.

At a relatively low heat treatment (300–450 °C) the loss of small molecules is the predominant factor determining the CC/CN ratio. The formation of the heterocyclic aromatic structure in this temperature range should not alter the CC/CN ratio. The major structural changes occurring at higher temperatures (750 °C) include nitrogen elimination and crosslinking of the one-dimensional ring structure both of which increase the CC/CN ratio. Thus the measured CC/CN ratios are in agreement with the proposed structures outlined in previous studies [31]. The CC/CN bonding ratio as estimated from the Cls spectrum of the ion-implanted sample (PAN435I) is surprisingly low (4.8) in view of the fact that the nitrogen content is only 2% (Table 1). Furthermore, the ratio is almost equal to that of PAN750 (4.2:1) for which the nitrogen content is 9%. The conclusions that can be drawn from these results are: (1) ion implantation causes extensive nitrogen depletion and (2) the nitrogen chemical state in the implanted sample is different from that found in the pyrolyzed material. To account for the low CC/CN ratio, I propose that the nitrogen bonding configuration in the implanted sample is such that a maximum number of C–N bonds per nitrogen atom is produced. This maximum number of C–N bonds must also be higher than the number of carbon to nitrogen bonds per nitrogen (C–N bonds/nitrogen) found in PAN750. This can be further explained as follows.

At temperatures above 600 °C, the denitrogenation of PAN is accompanied by the formation of a polyconjugated graphite-like structure [34]. Since a heteroatom in the center of such a polyconjugated structure will tend to destabilize the system, it is highly unlikely that a large number of these atoms will remain in those positions. Therefore, the majority of the residual nitrogen atoms are more likely present at the boundaries of the growing graphitic structure either in a heteroaromatic or in the form of dangling bonds [31]. The number of C–N bonds/nitrogen in such structures is expected to be smaller than that for systems in which the nitrogen atoms are located in the center of the polyconjugated structure. Thus the experimentally measured CC/CN ratio for PAN750 would decrease if the nitrogen atoms were to be positioned inside the growing graphite structure since there would be more C–N bonds per nitrogen atom. The low CC/CN ratio in the ion-implanted sample can then be explained in terms of structural rearrangements induced by the energetic ions. The primary result of ion irradiation is the formation of ions and radicals through ionization. These highly energetic species then react to produce new chemical bonds and structures. It is proposed that the new structure contains a greater number of C–N bond/nitrogen than either PAN435 or PAN750. This is consistent with the small CC/CN ratio observed in ion-implanted PAN435.

The N ls spectra of the various samples provided further information on the chemical environment of the nitrogen atoms. The spectra of PAN435 and PAN350 (not given in text) show a broad peak at a binding energy of 399.0 ± 0.2 eV corresponding to nitrogen in a heterocyclic aromatic structure. The N ls binding energy

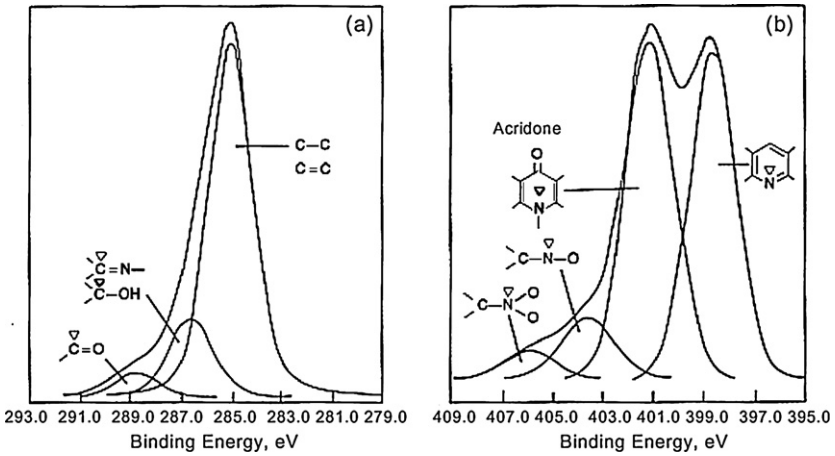

Fig. 4. Curve-resolved XPS (a) C 1s and (b) N 1s spectra of PAN750.

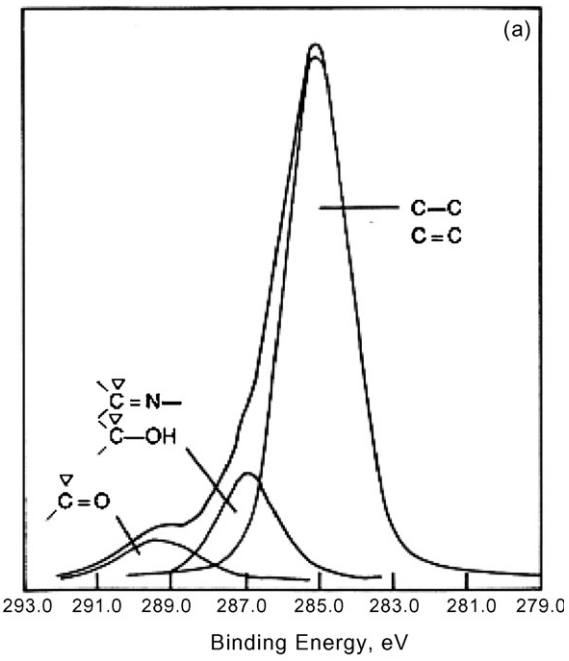

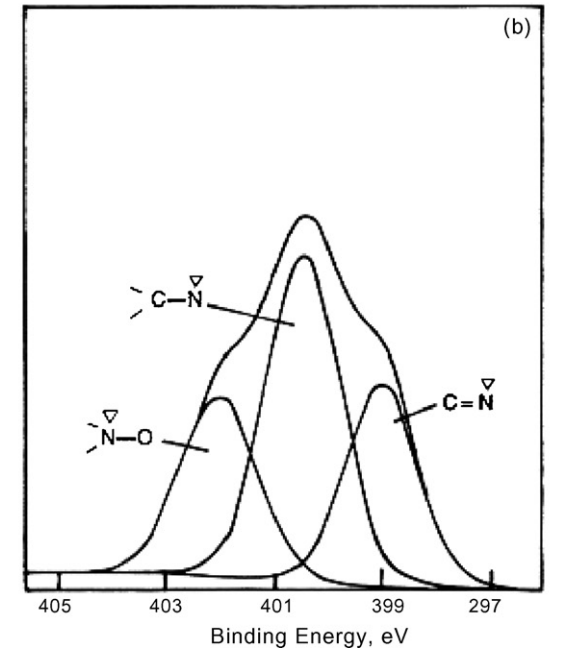

Fig. 5. Curve-resolved XPS (a) C 1s and (b) N 1s spectra of PAN750I.

of the model compound acridine 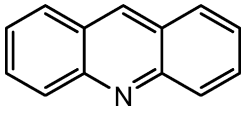 399 eV

[33], which is in excellent agreement with that found for PAN435 and PAN350 [32]. The N ls spectra of PAN750 and of PAN750I are given in Fig. 5a and b. The spectrum of PAN750 shows two distinctive peaks with a long tail extending into the higher energy side of the spectrum. The spectrum was curve-resolved into four components with binding energies of 398.6, 401.2, 403.7, and 406 eV. The major component (45% intensity) at the binding energy of 401.2 eV is assigned to a sigma bonded nitrogen atom based on a comparison with the N ls binding energy of 400.3 eV of the model compound quinacridone [33]. The component at the binding energy of 398.6 eV (42% intensity) is assigned to a nitrogen in a heteroaromatic structure as in the case of the pyrolyzed samples. The two smaller peaks at the high-energy side are due to the surface oxidation of the material. They are attributed to nitrogen atoms in aminoxide ($N \rightarrow 0$) and nitroxide ($-NO_2$) like structures [32]. Upon ion implantation, the component assigned to the nitrogen in a sigma bonding state (401.2 eV) increased in intensity (46%) relative to the intensity (27%) of the component for which the nitrogen is in a heteroaromatic structure (Fig. 5b). These observations lead further support to the conclusion that the chemical structures of the ion implanted and of the pyrolyzed samples are different. In the above calculations I have made the assumption that the extent and the nature of surface oxidation are the same in all specimens. A more thorough calculation would require the estimation of the contribution of oxidized carbon and nitrogen atoms to the overall N ls and C ls spectra. Sputtering of the near surface layer with argon ion would eliminate the oxygen contribution, but it will also induce undesirable structural rearrangements in the material. A dramatic decrease in the N ls Auger electron signal was observed due to a preferential sputtering of the nitrogen.

References

[1] T.H. Ko, H.Y. Ting, C.H. Lin, J. Appl. Polym. Sci. 35 (1988) 631–640.
[2] T.H. Ko, H.Y. Tin, C.H. Lin, J. Appl. Polym. Sci. 37 (1989) 553–566.
[3] O.P. Bahl, R.B. Mathur, T.L. Dhami, Mater. Sci. Eng. 73 (1985) 105–112.
[4] E. Fitzer, W. Frohs, M. Heine, Carbon 24 (1986) 387–395.
[5] R.J. Martin, W.J. Ng, Water Res. 19 (1985) 1527–1535.
[6] T.H. Ko, P. Chiranairadul, C.H. Lin, J. Mater. Sci. Lett. 11 (1992) 6–8.
[7] K. Kaneko, C. Ishii, M. Ruike, H. Kuwabara, Carbon 30 (1992) 1075–1088.
[8] M.K. Jain, A.S. Abhiraman, J. Mater. Sci. 22 (1987) 278–300.
[9] M.K. Jain, M. Balasubramanian, P. Desai, A.S. Abhiraman, J. Mater. Sci. 22 (1987) 301–312.
[10] T.H. Ko, S.C. Liu, J. Mater. Sci. Lett. 7 (1988) 628–630.
[11] T.H. Ko, P. Chiranairadul, J. Mater. Res. 10 (1995) 1969–1976.
[12] E. Fitzer, Acta Polym. 41 (1990) 381–389.
[13] L. Mascia, E.G. Paxton, Thermochim. Acta 184 (1991) 251–267.
[14] Y. Sugahara, K. Kuroda, C. Kato, J. Am. Ceram. Soc. 67 (1984) C247–C248.
[15] J.S. Tsai, J. Mater. Sci. Lett. 11 (1992) 140–142.
[16] E. Volpert, J. Selb, F. Candau, N. Green, J.F. Argillier, A. Audibert, Langmuir 14 (1998) 1870–1879.
[17] L. Sarvaranta, J. Appl. Polym. Sci. 56 (1995) 1085–1091.
[18] D. Eichenauer, H. Jung, Adv. Mater. 4 (1992) 215–220.
[19] B.A. Keller, Ch. Lowe, R. Hany, Surf. Interface Anal. 22 (1994) 284–289.
[20] N. Grassie, R. McGuchan, Eur. Polym. J. 6 (1970) 1272–1291.
[21] J.N. Hay, Thermal reactions of polyacrylonitrile, J. Polym. Sci. A l6 (1968) 2127–2135.
[22] J.W. Johnson, W.D. Potter, P.G. Rose, G. Scott, Br. Polym. J. 4 (1972) 527.
[23] G. Oguz, J. Hacaloglu, A. Onal, J. Macromol. Sci. A 42 (2005) 1387–1397.
[24] G.E. Wneck, B. Wasserman, M.S. Dresselhaus, S.E. Tunney, J.K. Stille, Polym. Sci.: Polym. Lett. Ed. 23 (1985) 609–612.
[25] T. Vankatesan, R.C. Dynes, B. Wilkens, A.E. White, J.M. Gibson, R. Hamm, Nucl. Inst. Methods: Phys. Res. B 1 (1984) 599–605.
[26] H. Tsuji, H. Satoh, S. Ikeda, N. Ikenoto, Surf. Coat. Technol. 103/104 (1998) 124–128.
[27] J. Linhard, M. Scharff, H.E. Schiott, K.D. Vidensk, Mat. Fys. Medd. Dan. Vidensk. Selsk 33 (1963) 14–29.
[28] V.P. Tolstoy, Handbook of Infrared Spectroscopy of Ultrathin Films, John Wiley and Sons Inc., 2003.
[29] H. Toech, P.D. Metz, W.G. Wilhelm, Mol. Cryst. Liquid Cryst. 83 (1982) 297–302.
[30] A.R. Monahan, J. Polym. Sci. A 4 (1966) 2391–2399.
[31] J.R. Pels, F. Kapteijn, J.A. Moulijn, Q. Zhu, K.M. Thomas, Carbon 33 (1995) 1641–1653.
[32] D.T. Clark, H.R. Thomas, J. Polym. Sci.: Polym. Chem. Ed. 16 (1978) 791–820.
[33] T. Takahagi, I. Shimada, M. Fukuhara, K. Morita, A. Ishitani, J. Polym. Sci.: Polym. Chem. Ed. 24 (1978) 3101–3107.
[34] S. Kazawa, T. Hashimoto, A. Takaku, Synth. Met. 14 (1986) 153–164.